Richardson, J. S., & Richardson, D. C. (1988) *Science 240*, 1648–1652.
Query, C. C., Bentley, R. C., & Keene, J. D. (1989) *Cell 57*, 89–101.
Sachs, A. B., Bond, M. W., & Kornberg, R. D. (1986) *Cell 45*, 827–835.
Saito, H., & Ando, I. (1989) *Annu. Rep. Nucl. Magn. Reson. Spectrosc. 21*, 251–263.
Sambrook, J., Fritsch, E. F., & Maniatis, T. (1989) *Molecular Cloning, A Laboratory Manual*, Cold Spring Harbor Laboratory, Cold Spring Harbor, New York.
Saudek, V., Williams, R. P. J., & Ramponi, G. (1989a) *FEBS Lett. 242*, 225–232.
Saudek, V., Atkinson, R. A., Williams, R. P. J., & Ramponi, G. (1989b) *J. Mol. Biol. 205*, 229–239.
Scherly, D., Boelens, W., van Venrooji, W. J., Dathan, N. A., Hamm, J., & Mattaj, I. W., (1989) *EMBO J. 8*, 4163–4170.
Scherly, D., Boelens, W., Dathan, N. A., van Venrooij, W. J., & Mattaj, I. W. (1990) *Nature 345*, 502–506.
Shaka, A. J., Keeler, J., Frenkiel, T., & Freeman, R. (1983) *J. Magn. Reson. 52*, 335–338.
Shaka, A. J., Barker, P. B., & Freeman, R. (1985) *J. Magn. Reson. 64*, 547–552.
Shaka, A. J., Lee, C. J., & Pines, A. (1988) *J. Magn. Reson. 77*, 274–293.
Spera, S., & Bax, A. (1991) *J. Am. Chem. Soc. 113*, 5490–5492.
States, D. J., Haberkorn, R. A., & Ruben, D. J. (1982) *J. Magn. Reson. 48*, 286–292.
Studier, F. W., Rosenberg, A. H., Dunn, J. J., & Dubbendorf, J. W. (1990) *Methods Enzymol. 185*, 60–89.
Swanson, M. S., & Dreyfuss, G. (1988a) *Mol. Cell. Biol. 8*, 2237–2241.
Swanson, M. S., & Dreyfuss, G. (1988b) *EMBO J. 11*, 3519–3529.
Swanson, M. S., Nakagawa, T. Y., LeVan, K., & Dreyfuss, G. (1987) *Mol. Cell. Biol. 7*, 1731–1739.
Wüthrich, K. (1986) *NMR of Proteins and Nucleic Acids*, John Wiley and Sons, New York.
Zhu, G., & Bax, A. (1990) *J. Magn. Reson. 90*, 405–410.
Zuiderweg, E. R. P., & Fesik, S. W. (1989) *Biochemistry 28*, 2387–2391.

Pulsed EPR Studies of the Type 2 Copper Binding Site in the Mercury Derivative of Laccase†

Jinfeng Lu,‡,§ Christopher J. Bender,‡ John McCracken,‡,∥ Jack Peisach,*,‡ John C. Severns,⊥ and David R. McMillin*,⊥

Department of Molecular Pharmacology, Albert Einstein College of Medicine of Yeshiva University, 1300 Morris Park Avenue, Bronx, New York 10461, and Department of Chemistry, Purdue University, West Lafayette, Indiana 47907

Received March 2, 1992; Revised Manuscript Received April 27, 1992

ABSTRACT: The nuclear modulation effect in pulsed EPR spectroscopy was used to study the type 2 copper binding site in the mercury derivative of laccase (MDL) in which the type 1 copper is substituted by Hg(II). By comparing the three-pulse electron spin–echo modulations and Fourier transform spectra of MDL and several model compounds, we conclude that the imidazole groups of two histidyl amino acid residues are equatorially coordinated to Cu(II) in the type 2 site. Computer simulations of these data suggest that the remote nonbonding nitrogens of the two imidazoles possess nuclear quadrupole parameters e^2qQ = 1.47 MHz and η = 0.83. A_{iso} values of these two nitrogens are not identical, being 1.5 and 2.0 MHz. We have also used samples of the enzyme exchanged with D_2O to examine the coordination of the water to the type 2 copper site. The deuterium modulation that is resolved by taking the ratio of the time domain ESEEM data from native and D_2O-exchanged enzyme indicates that there is an equatorial water ligand, and further data show that this water is displaced by azide.

Laccase is an intensely blue, copper-containing protein found in plants and fungi (Reinhammar, 1984). It catalyzes the oxidation of aromatic diamines and diphenols, yielding water as the final product of dioxygen reduction. The intense blue color arises from a thiolate to Cu(II) charge transfer at one of the metal sites (McMillin et al., 1974; Solomon et al., 1976a,b). This site, termed type 1 (Malmstrom et al., 1968), has an unusually small nuclear hyperfine coupling constant, $A_\parallel$, in the EPR.[1] On the basis of optical and magnetic properties, it resembles some low molecular weight, mononuclear copper proteins where the copper is bound to a cysteinyl sulfur, two histidyl imidazoles, and a methionyl sulfur (Colman et al., 1978; Adman et al., 1978; Norris et al., 1981). Imidazole coordination is demonstrated by pulsed EPR methods (Mondovi et al., 1977; Avigliano et al., 1981). The

† This work supported by National Institute of General Medical Sciences Grant GM 40168 and NIH Grant RR-02583 (J.P.) and GM 22764 from the U.S. Public Health Service (D.M.).

* Authors to whom correspondence should be addressed.
‡ Einstein College of Medicine.
§ Present address: National Laboratory of Natural and Biomimetic Drugs, Beijing Medical University, Beijing 100083, People's Republic of China.
∥ Present address: Department of Chemistry, Michigan State University, East Lansing, MI 48824-1322.
⊥ Purdue University.

[1] Abbreviations: EPR, electron paramagnetic resonance; ESEEM, electron spin–echo envelope modulation; ENDOR, electron–nuclear double resonance; MDL, mercury derivative of laccase; LEFE, linear electric field effect; NQI, nuclear quadrupole interaction; EXAFS, extended X-ray absorption fine structure spectroscopy.

0006-2960/92/0431-6265$03.00/0

Hg(II) EXAFS spectrum of a laccase derivative with Hg(II) incorporated into the type 1 site reveals the presence of two histidyl imidazole ligands and a sulfur ligand bound to the metal (Klemens et al., 1989).

A second Cu(II) site in laccase, termed type 2, is characterized from its magnetic properties as resembling those in Cu(II) amino acid and peptide complexes but having no sulfur coordinated to the metal (Peisach and Blumberg, 1974). Imidazole coordination has been demonstrated by pulsed EPR here as well (Mondovi et al., 1977). Moreover, nitrogen superhyperfine structure has been resolved in the S-band EPR spectrum of the type 2 copper center when mercury is bound to the type 1 site (Morie-Bebel et al., 1986).

The third copper site, termed type 3, consists of a spin-coupled binuclear Cu(II) pair (Reinhammar, 1972; Solomon et al., 1976a,b) that makes no contribution to the EPR properties of the protein.

The integrity of each copper site in laccase is necessary for catalytic activity. Therefore, removal of type 2 copper (Graziani et al., 1976) or substitution of the type 1 copper ion by mercury (Morie-Bebel et al., 1984) disrupts enzyme function. Activity is also inhibited by the binding of anions such as fluoride or azide (Branden et al., 1973).

The EPR spectra of type 1 and type 2 copper overlap, and this renders structural analysis of the individual sites difficult. For this reason, one must either reversibly remove one of the paramagnetic copper atoms, such as the type 2 copper (Graziani et al., 1976), or substitute the type 1 copper with an EPR silent surrogate, such as Hg(II) (Morie-Bebel et al., 1984). It is this latter procedure that has afforded us the opportunity to characterize the type 2 site without interference from type 1 copper using ESEEM spectroscopy. This pulsed EPR method is particularly useful for the elucidation of structure in the vicinity of paramagnetic centers based on the analysis of weak superhyperfine interactions (Mims & Peisach, 1989). With this procedure, we demonstrate that for laccase where Hg(II) is substituted in the type 1 center there are at least two imidazole nitrogen atoms coordinated to type 2 copper and that in the D_2O exchanged sample water is coordinated to copper and this is displaced when azide, an enzyme inhibitor of the native protein, is bound.

Materials and Methods

Diethylenetriamine (97% Fluka AG) and cupric acetate (Fisher Scientific) were used without further purification. Imidazole (Eastman) was recrystallized from chloroform prior to use. $Na^{15}N_3$ was obtained from Prochem.

The mercury derivative of laccase was prepared as described by Morie-Bebel et al. (1984). Here, the apoprotein from *Rhus vernicifera* was reconstituted with Hg occupying the type 1 site and ^{63}Cu at the type 2 and type 3 sites. For magnetic measurements the enzyme was in 0.1 M phosphate buffer, pH 6, and its concentration, estimated from the copper content, was approximately 2 mM. D_2O exchange of the enzyme was carried out by diluting the protein 5-fold with phosphate buffer in D_2O, concentrating by ultrafiltration, and repeating this procedure twice.

The azide derivative of the enzyme was prepared by adding a 15-fold molar excess of $Na^{15}N_3$.

Mono-, bis-, and tris(bipyridyl) complexes of Cu(II) were prepared following procedures already described (McCracken et al., 1987), as was copper(II) diethylenetriamine imidazole (Mims & Peisach, 1978). A copper(II) bis(imidazole) complex was formed by dissolving 4 mM copper(II) oxalate with 32 mM imidazole at neutral pH; copper(II) tetrakis(imidazole) was likewise formed from 5 mM copper acetate to which 200 mM imidazole was added. The solvent system used for model experiments was ethylene glycol/water or ethylene glycol/D_2O (1:1 v/v).

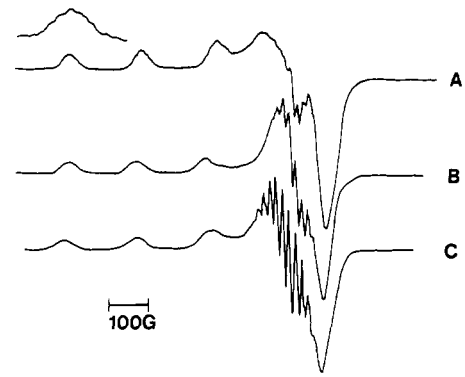

FIGURE 1: X-band EPR spectra of the mercury derivative of laccase and of two copper(II) imidazole complexes: (A) enzyme; (B) copper(II) oxalate bis(imidazole); (C) copper(II) tetrakis(imidazole). Spectrometer conditions: microwave power, 5 mW; microwave frequency, 9.10 GHz; field modulation amplitude, 5 G; temperature, 77 K.

The pulsed EPR spectrometer used for these experiments has been described before (McCracken et al., 1987). However, the traveling wave tube amplifier has since been modified to reduce the gating fall time and to provide some reduction in amplifier noise. A reflection cavity that contains a folded stripline element as the resonant structure (Lin et al., 1985; Britt & Klein, 1988) was used. As configured, the spectrometer had a deadtime of 70–80 ns. Two- and three-pulse electron spin–echo data were obtained at X-band at 4.2 K. The three-pulse experiments were performed with a τ value selected for suppression of the proton Larmor line (i.e., $\tau = n/\nu_H$; $n = 2, 3$). Typical microwave pulse powers were 50 W delivered in a 12-ns pulse. The repetition rate of the applied pulse sequence was 100 Hz. Nuclear modulation data lost to instrumental deadtime was reconstructed using a procedure developed by Mims (1984) and which is part of a software package written by us that also includes routines for fast Fourier transformation and the rationing of two time domain traces.

Results and Discussion

EPR Spectra. The X-band EPR spectrum of the mercury derivative of laccase at 77 K is shown in Figure 1A. The line shape, characteristic of EPR spectra for type 2 copper (Morie-Bebel et al., 1986), is typical for Cu(II) centers having near axial symmetry, with principal g values of $g_\perp = 2.05$ and $g_\parallel = 2.25$. The copper hyperfine content $A_\parallel$ is about 575 MHz. One notes a poorly resolved, multiline superhyperfine pattern at $g_\perp$, which suggests that nitrogens are coordinated to Cu(II). The number of superhyperfine lines that, in theory, can be resolved for the coupling of a nuclear spin I to an electron $S = {}^1/_2$ is given by the expression $2In + 1$, where n is the number of coupled nuclei. However, counting lines at the $g_\perp$ feature of the spectrum as a means of determining the number of ^{14}N bound to Cu(II) may yield an overestimate since the spectral line shape may not reflect purely axial symmetry, and one would expect contributions from both g_x and g_y.

A more accurate count of superhyperfine lines is generally obtained at the low-field ($M_s \approx -{}^1/_2$) hyperfine feature of the Cu(II) spectrum. In many cases, the spectral resolution at X-band is poor because of strain broadening, and one resorts to measurements at S-band, where resolution is sometimes improved (Hyde & Froncisz, 1982; Froncisz & Aisen, 1982). Such an S-band measurement was made for the mercury

derivative of laccase, where a poorly resolved, multiline pattern on the $M_s = -1/2$ transition is reported. Although this spectral feature was simulated with a seven-line superhyperfine pattern assuming electron nuclear coupling with three equivalent ^{14}N, seven distinct lines are not clearly evident in the spectrum (Morie-Bebel et al., 1986; Figure 4).

For comparison purposes, X-band EPR spectra of copper(II) oxalate bis(imidazole) (Figure 1B) and copper(II) tetrakis(imidazole) (Figure 1C) are also illustrated. These spectra have characteristic features of $g_\parallel = 2.28$, $A_\parallel = 535$ MHz and $g_\parallel = 2.24$, $A_\parallel = 610$ MHz, respectively. In general, an increase of the number of coordinated nitrogens at the expense of coordinated oxygens may result in an increase in the number of superhyperfine lines observed in the spectrum and, more usually, an increase in the magnitude of $A_\parallel$ and a decrease in the value of $g_\parallel$, provided that the site symmetry is regular (Blumberg & Peisach, 1987). On the basis of the magnitude of $A_\parallel$ and $g_\parallel$, it was suggested (Morie-Bebel et al., 1986) that the ligand coordination for the type 2 copper in the mercury derivative of laccase is probably of the type 3N1O. However, changes in ligand charge as well as site symmetry preclude accurate assignments that are able to differentiate 2N2O, 3N1O, and 4N type ligation (Peisach & Blumberg, 1974). Therefore, as a means of further elucidating the coordination site, we turn to electron spin–echo experiments to determine the ligand structure about the metal ion.

Couplings of Amino or Remote Nitrogens from Coordinated Imidazoles. On the basis of the purported seven-line splitting of the $M_s = -1/2$ feature in the EPR spectrum of the mercury derivative of laccase at S-band, it has been suggested that there are three nitrogens coordinated to the type 2 Cu(II) site (Morie-Bebel et al., 1986). If these are all the directly coordinating nitrogens of bound imidazole, they will not contribute to the electron spin–echo envelope modulations (Mims & Peisach, 1978) because the couplings are larger than the frequency range that can be covered in a spin–echo experiment. The remote nitrogen of bound imidazole is more weakly coupled to the copper, and it is this nitrogen that contributes to the echo envelope modulation that is observed.

In general, the Hamiltonian expression for the weakly coupled nitrogens consists of three terms corresponding to (i) the nuclear Zeeman interaction, (ii) the electron–nuclear superhyperfine interaction, and (iii) the nuclear quadrupole interaction (NQI). This Hamiltonian can be written

$$H = H_{\text{nuc Zeeman}} + H_{\text{shf}} + H_{\text{Q}} \quad (1)$$

At an applied field of approximately 3000 G the superhyperfine interaction nearly cancels the nuclear Zeeman interaction of the remote nitrogen of Cu(II)-coordinated imidazole, and the Hamiltonian is essentially simplified to that of the quadrupole term for one of the electron spin manifolds. Under these conditions we expect to observe only the three zero field quadrupole frequencies ν_-, ν_0, and ν_+, which are related to the electric field gradient parameters as follows:

$$\nu_\pm = 3/4(1 \pm 1/3\eta)(e^2Qq) \quad (2)$$

$$\nu_0 = 1/2\eta(e^2Qq) \quad (3)$$

Here, e^2Qq is the nuclear quadrupole interaction and η the asymmetry parameter.

The frequency spectrum obtained from the Fourier transform of the three-pulse echo modulation data shown in Figure 2 contains three intense lines at 0.74, 1.51, and 3.90 MHz, plus other features. We interpret our data as done previously by Mims and Peisach (1978); that is, the nuclear modulation frequencies identified at 0.74 and 1.51 MHz correspond to the zero field nuclear quadrupole frequencies of the spin manifold in which the Zeeman and hyperfine energies cancel. [Previous studies have indicated that the observed 0.74-MHz line is a composite of two nuclear quadrupole lines (Mims & Peisach, 1978; Jiang et al., 1990).] The frequency at 3.9 MHz is assigned to the double quantum transition from the other spin manifold in which the Zeeman and contact terms add.

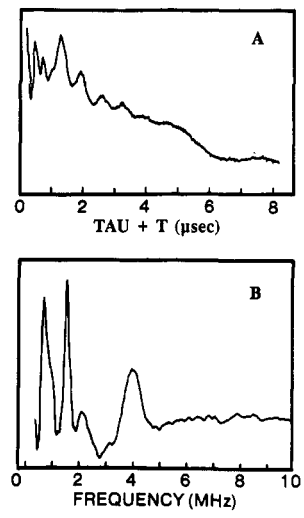

FIGURE 2: Three-pulse electron spin–echo modulation (A) and the Fourier transform (B) for the mercury derivative of laccase. Spectrometer conditions: microwave frequency, 8.9 GHz; microwave power, 63 W; applied magnetic field, 3000 G; τ, the spacing between the first and second microwave pulses, 156 ns; temperature, 4.2 K; the echo envelope is obtained in 1000 points over the time interval indicated on the abscissa.

When two or more magnetically equivalent ^{14}N nuclei give rise to lines in a spin–echo spectrum, combination frequencies are observed (Kosman et al., 1980; McCracken et al., 1988). In the spectrum shown in Figure 2, two lines at 2.25 and 3.0 MHz are seen, and these can be assigned to combination frequencies of the nuclear quadrupole lines at 0.74 and 1.5 MHz. The presence of these combination lines indicates that more than a single imidazole is coordinated to Cu(II), in accord with the CW EPR result. We can use the amplitudes of these combination lines relative to the "fundamental" frequencies as a means of quantifying the number of imidazoles bound.

The above arguments are reinforced by the ESEEM spectra of three model compounds illustrated in Figure 3. Here, we compare the spectra of copper(II) diethylenetriamine imidazole, copper(II) oxalate bis(imidazole), and copper(II) tetrakis(imidazole), in which Cu(II) is coordinated to one, two, and four imidazoles, respectively. As was the case for the mercury derivative of laccase, these spectra all have characteristic frequency components near 0.58–0.78, 1.46, and 4 MHz. For those complexes that contain more than a single imidazole ligand, combination frequencies near 2.0–2.3 and 2.9 MHz are evident. The relative amplitudes and line width of the combination frequencies with respect to the double quantum transition (4 MHz) can be seen to increase with the number of imidazoles coordinated (McCracken et al., 1988). From a comparison of these features with those present in the laccase spectrum (Figure 2), we conclude that there are at least two imidazoles coordinated to the type 2 copper site in the enzyme.

Simulations of ^{14}N Modulations. To further examine the nuclear modulations of the remote or amino nitrogen of copper-coordinated imidazole and the effects of multiple equivalent nuclei on these modulations, we turn to ESEEM simu-

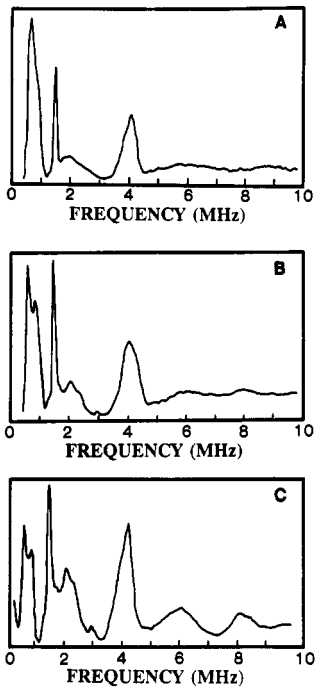

FIGURE 3: Frequency spectra of three copper(II) imidazole complexes obtained from Fourier transformation of three pulse ESEEM data: (A) copper(II) diethylenetriamine imidazole; (B) copper(II) oxalate bis(imidazole); (C) copper(II) tetrakis(imidazole). Spectrometer conditions: microwave frequency, 8.8 GHz; microwave power, 63 W; applied magnetic field, 3065 G; τ, 230 ns; temperature, 4.2 K; data recorded as described in the caption of Figure 2.

lation techniques (Cornelius et al., 1990) that are based upon the density matrix formalism of Mims (1972). The form of the Hamiltonian operator used in these simulations is

$$H_N = SA_NI - g_N\beta_N\mathbf{B}I + (e^2qQ/4)[3I_z^2 - 2 + \eta(I_x^2 - I_y^2)] \quad (4)$$

To perform the simulations, 11 parameters are required. If the electron–nuclear hyperfine coupling tensor is constrained to be axial, only two coupling parameters and two angles relating the relative orientation of A_N to the g-tensor are needed. This reduces the number of variables in the above expression to nine. The other five variables are those needed to describe the nuclear quadrupole interactions: e^2qQ, the quadrupole coupling constant; η, the asymmetry parameter; and the three Euler angles that are needed to relate the principal axes of the tensor to the g-tensor.

The simulation procedure starts by selecting the Euler angles and rotating the nuclear quadrupole interaction operator. The Hamiltonian matrix is then calculated for both electron spin sublevels using the effective NQI parameters and the remainder of the nuclear Zeeman term. The values of e^2Qq and η are then optimized to provide a best fit of the low-frequency components of the spectrum, which, to a good approximation, are solely dependent upon the nuclear quadrupole interaction. Likewise, the frequency of the simulated double quantum transition at approximately 4 MHz is optimized by adjusting the isotropic portion of the nuclear hyperfine interaction; anisotropic terms of the hyperfine tensor are then varied to fit line shape and width. Finally, the simulated modulation patterns are multiplied by an exponential function $[\exp(-t/\tau)]$ to account for the decay of the echo amplitude due to relaxation processes.

Simulations of a three-pulse spin–echo data set performed at 8.8 GHz and an applied field of 3065 G were carried out. For ^{14}N the nuclear g value was taken as 0.40349. The

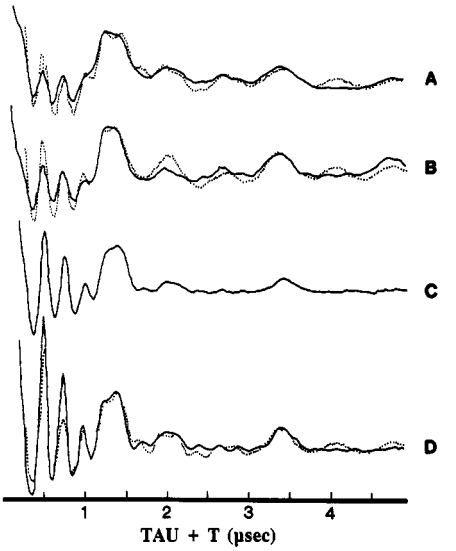

FIGURE 4: Simulation of three-pulse echo envelope modulations for Cu(II) coordinated by one (A), two (B), three (C), and four (D) imidazoles. The solid lines indicate the simulated data, and the dotted lines correspond to the experimental modulation data for the samples described in Figure 3. Simulation parameters: $g_n = 0.40349$; $\theta_n = 90°$; $\psi_n = 0°$; $e^2Qq = 1.47$; $\eta = 0.83$; $\alpha = 75°$; $\beta = 90°$; $\gamma = 0°$; $A_{iso} = 2.02$ (A), 2.04 (B), 2.07 (C), 2.10 MHz (D); $r = 2.7$ Å; 512 points were used in the simulation.

modulation pattern was simulated for a fixed τ value of 230 ns, and data points were obtained at 10-ns intervals. The results of the simulation and the relevant experimental modulation patterns are illustrated in Figure 4 for copper coordinated to one, two, three (theoretical fit), and four imidazoles (A–D, respectively).

As would be expected from theory, the frequencies of the nuclear quadrupole lines are primarily determined by the values of e^2Qq and η, whereas the amplitude of these features is sensitive to the relative orientation of the nuclear quadrupole tensor and the g-tensor (McCracken et al., 1988). In our simulations, the values that gave optimal agreement with experiment were $e^2Qq = 1.47$ MHz and $\eta = 0.83$. These parameters gave modulation periodicities of 1.72, 1.16, and 0.68 μs, which corresponds to frequencies of 0.58, 0.86, and 1.47 MHz, respectively. The Euler angles that gave these results were $\alpha = 75$, $\beta = 90$, and $\gamma = 0$.

The electron–nuclear hyperfine coupling tensor is described using a point dipole model, which is then added directly to the isotropic term. The hyperfine tensor is thus parameterized by **r**, the effective electron–nuclear distance, and angles θ_n and θ_n, which describe the rotations of the hyperfine tensor principal axis from that of the g-tensor. Best fits of the double quantum frequency component for the remote or amino nitrogen of copper complexes containing one, two, and four imidazoles are obtained using isotropic hyperfine coupling terms of 2.02, 2.04, and 2.10 MHz, respectively. The resultant frequencies obtained using these input parameters are 4.04, 4.06, and 4.14 MHz (cf. Figures 3 and 4). For the simulation of the tris(imidazole) coordinated copper complex, for which we have no experimental data, A_{iso}, the isotropic hyperfine coupling constant, for the amino nitrogen was selected to be an intermediate value 2.07 MHz, and we obtained a double quantum transition at 4.11 MHz in this simulation.

We also simulated the frequency spectrum of the three-pulse experiment performed on the mercury derivative of laccase. The low-frequency components of the spectrum differ slightly from those of the model compounds, and the best fit of the simulation to the enzyme data was obtained by simply read-

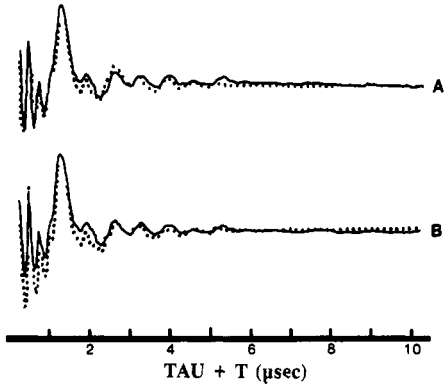

FIGURE 5: Simulation of the three-pulse echo envelope modulation data for the mercury derivative of laccase (solid line) and comparison with experiment (dotted line): (A) simulation assuming two nonequivalent nitrogens; (B) simulation assuming two equivalent nitrogens and a third nonequivalent nitrogen. The solid line indicates experimental data; the dotted line is the simulated modulation. For the experimental data, spectrometer conditions are as described in Figure 3. Simulation parameters: $e^2Qq = 1.47$; $\eta = 0.91$; $\alpha = \beta = \gamma = 0°$; $r = 2.6$ Å (all other parameters as in Figure 4). A_{iso} for the weakly coupled nitrogen is 1.5 MHz; the more strongly coupled nitrogen is fit with an A_{iso} of 2.0 MHz.

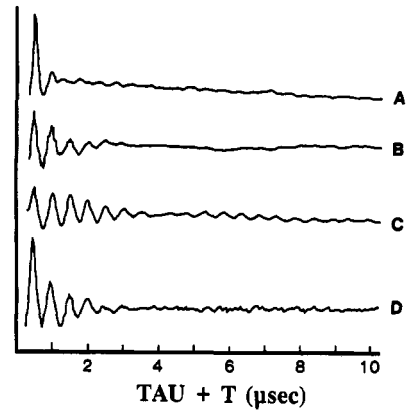

FIGURE 6: Three-pulse modulation data obtained by a ratio procedure for (A) equatorially and (B) axially coordinated D_2O ligated to Cu(II) in a model study with copper(II) mono-, bis-, and tris(bipyridyl) complexes in D_2O and H_2O; (C) three-pulse deuterium modulation data for ambient water outside the coordination sphere of copper(II) tris(bipyridyl). Trace D is the ratio of modulation data for the mercury derivation of laccase studied in D_2O and in H_2O. Trace A is the ESEEM pattern obtained by dividing the ratio of envelope modulations for Cu(II)bpy in D_2O and in H_2O by the ratio of envelopes for $Cu(II)(bpy)_2$ in D_2O and in H_2O. The modulation shown is from two D_2O coordinated equatorially to Cu(II). Trace C was obtained by taking the ratio of modulation envelopes for $Cu(II)(bpy)_3$ in D_2O and in H_2O by the ratio of envelopes for $Cu(bpy)_3$ in D_2O and in H_2O. The modulation shown is from two D_2O coordinated axially to Cu(II). Trace B was obtained by dividing the modulation data for $Cu(II)(bpy)_2$ in D_2O by that in H_2O, leaving the modulation from ambient water. Experimental conditions were as described in Figure 3. For a discussion of the rationale for the models chosen, see McCracken et al. (1987).

justing the quadrupole coupling terms to $e^2Qq = 1.47$ MHz and $\eta = 0.91$. For the 4-MHz peak, however, the experimental data suggest that the feature here might be due to a contribution from two sources; that is, there seem to be two overlapping peaks from amino nitrogens with presumably slightly different isotropic couplings. We attempted to mimic these feature by performing simulations of complexes containing two and three nonequivalent (with respect to the nuclear hyperfine coupling) imidazoles. In these simulations isotropic coupling constants of 1.5 and 2.0 MHz were used; Figure 5A is the simulated echo envelope of a complex containing two nonequivalent imidazoles, and Figure 5B is the result obtained when two weakly coupled (1.5 MHz) imidazoles and one more strongly coupled (2.0 MHz) imidazole are coordinated to the copper. A comparison of these two simulations with the experimental data indicates that the best fit is attained for the model that features two nonequivalent imidazoles with A_{iso} differing by 0.5 MHz. We therefore conclude that two imidazoles are bound equatorially to the type 2 site.

As A_{iso} values for the remote nitrogens of the two coordinated imidazoles differ by about 25%, it is reasonable to assume that a similar difference in coupling will be observed for the directly coordinated nitrogens as well. For example, the two directly coordinated imidazole nitrogens in the copper protein stellacyanin show differences in coupling that vary by about 50% (Roberts et al., 1984). On the basis of ESEEM spectral simulation, the couplings of the two remote nitrogens are also shown to differ by about 50% (J. McCracken and J. Peisach, unpublished observations). Therefore, the continuous wave S-band EPR spectrum for the mercury derivative of laccase is expected to show neither a five-line superhyperfine pattern indicative of coordination to two equivalently coupled ^{14}N nor a seven-line pattern indicative of coordination to three equivalently coupled ^{14}N (Morie-Bebel et al., 1986; Figure 5). Inequivalent nitrogen coupling is suggested, and this would lead to the poor spectral resolution obtained.

Although it is clear from our ESEEM spectral simulations that at least two imidazoles are coordinated equatorially to copper, we are not able from our studies to determine whether another imidazole is coordinated axially. The modulations arising from an axially coordinated ^{14}N at X-band are so weak (Cornelius et al., 1990) that their spectral contributions cannot be resolved where two imidazoles are coordinated equatorially to Cu(II). Our experiments would also be an insensitive to a third equatorially coordinated nitrogen based ligand of a different origin (e.g., lysine).

Water as a Ligand to the Cu(II). The superhyperfine contribution of protons belonging to any water molecules that serve as ligands to the copper would be immeasurably small by conventional EPR spectroscopy, and we instead rely upon pulsed electron spin resonance techniques, which are better suited for the study of weak hyperfine interactions (Tsvetkov & Dikanov, 1987). To determine whether water molecules are bound as ligands to copper, we recorded spin–echo nuclear modulation envelopes for two mercuric laccase preparations, one of which was exchanged against D_2O.

The spin–echo modulation pattern that we observe for the mercury derivative of laccase comprises contributions from protons, nitrogens, and, following the appropriate substitution, deuterons. The total modulation of the electron spin–echo can be expressed mathematically as a product of the individual nuclear modulation components (Mims, 1972), so that

$$V_{mod}(I_1,I_2,...,I_n) = V_{mod}(I_1)V_{mod}(I_2)...V_{mod}(I_n) \quad (5)$$

Therefore, it follows that, if one wants to "subtract" contributions of a given component from the total modulation function, one needs to obtain the ratio of two modulation functions (Mims et al., 1984).

The ratio data of the corresponding experimental three-pulse echo modulation obtained from samples of MDL and three copper–bipyridyl complexes are illustrated in Figure 6A–D. Copper(II) mono-, bis-, and tris(bipyridyl) complexes have been selected as models for the comparative study of modulations from equatorially bound, axially bound, and ambient water on the basis of a study that demonstrated a means to selectively resolve the modulations of specifically coordinated water ligands from these complexes. The rationale of the

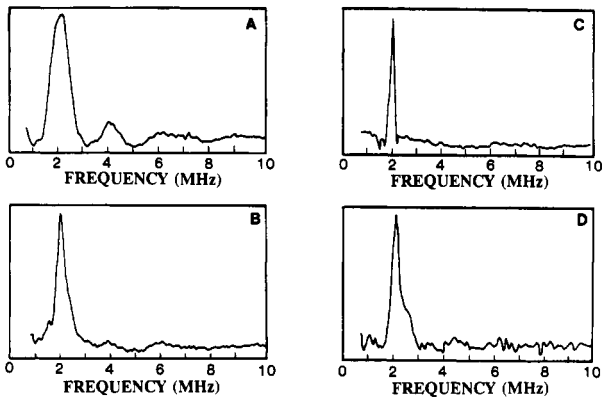

FIGURE 7: Fourier transforms of three-pulse echo envelope data for (A) equatorial and (B) axial D_2O, (C) ambient D_2O, and (D) deuterium interacting with the type 2 Cu(II) in laccase where Hg^{2+} is coordinated to the type 1 copper site. The modulation data sets used are shown in Figure 6.

chemistry and the various physical analyses of the structure are reviewed by McCracken et al. (1987) in an ESEEM study of the water ligated to amine oxidase.

The periodicity observed in the ratio of modulation data from native and D_2O-exchanged MDL arises from deuterium interaction and clearly shows that the type 2 Cu(II) site is accessible to water. A Fourier transform (Figure 7D) of the three-pulse modulation pattern shown in Figure 6D provides the frequency spectrum of the couplings of the deuterium to the electron spin of the Cu(II) in the protein. For the mercury derivative of laccase exchanged against D_2O the resolved deuterium modulation obtained by the ratio procedure comprises contributions from copper-coordinated D_2O, noncoordinated D_2O, and deuterium that has replaced exchangeable protons on the protein itself. All of these weakly coupled deuterons are identical to those termed "matrix" nuclei in the ENDOR spectroscopy literature [cf. Hyde et al. (1968) and Kevan and Kispert (1976)]. The spectrum obtained by Fourier transformation of the ratioed laccase data provides a composite of spectral features centered at the deuterium Larmor frequency near 2 MHz. The line can be resolved into a broad component and a narrow component arising from individual populations of nuclei with different hyperfine anisotropy or effective electron–nuclear distances. From a comparison of Fourier transforms of the modulation data for D_2O coordinated equatorially (Figure 7A) or axially (Figure 7B) to Cu(II) and in the ambient environment (Figure 7C), one notes that the relative line widths of the 2-MHz line differ. For those deuterons closest to the Cu(II), such as on an equatorial water molecule, the deuterium modulation pattern "damps" fastest (Figure 6A), resulting in a broad 2-MHz line in the Fourier transform. The damping of the population of deuterons furthest away, those in the ambient environment, is the slowest (Figure 6C), resulting in a narrow 2-MHz line (Figure 7C). For axially coordinated D_2O, the damping/line width is intermediate (Figures 6B and 7B).

On the basis of a comparison with Fourier transforms of modulation data for models (cf. Figure 7A–C) with that for the protein (Figure 7D), one can clearly recognize a broad component likely arising from deuterium in close proximity to the metal ion, as well as a narrow component from ambient deuterons. From this study it is suggested that water is a ligand to copper in laccase where mercury replaces type 1 copper. This finding is supported by the demonstration by Branden and Deinum (1977) that the EPR spectrum attributable to type 2 copper in laccase is broadened subsequent to the addition of $H_2{}^{17}O$.

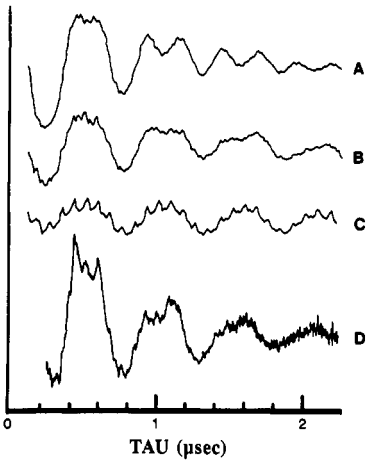

FIGURE 8: Two-pulse eacho envelope data for (A) equatorial, (B) axial, and (C) ambient D_2O obtained from the model study described in the legend to Figure 6. Trace D is the two-pulse deuterium data for the mercury derivative of laccase. The data shown are ratios obtained from studies of equivalent samples in D_2O and in H_2O. Experimental conditions are as described in Figure 2.

As an alternative method we can also determine the origin of the deuterium modulations from an analogous two-pulse electron spin–echo experiment (Figure 8). For deuterium, a second harmonic of the matrix nuclear frequency is generated by the sum of the two nuclear frequencies associated with the spin-up and spin-down states. Characteristics of the nuclear coupling affect the relative decay rates of the fundamental and second harmonic modulation amplitudes. In general, the second harmonic decays much more slowly than the fundamental because for the second harmonic the two nuclear transitions undergo opposite and nearly equal shifts in the field of the electron. For a nucleus of $I \geq {}^1/_2$, however, the quadrupole shift is independent of the electron spin orientation and will hasten the damping of this component. The line widths of the fundamental frequencies are mostly determined by the hyperfine anisotropy and will be strongly damped for close nuclei. As a result, the second harmonic for deuterium is difficult to observe in a two-pulse experiment unless the electron nuclear coupling is significantly greater than the quadrupole shift. The presence or absence of the second harmonic, then, provides a tool for distinguishing close or coordinated from noncoordinated water deuterons (McCracken et al., 1987).

From the results of the model compound study that are illustrated in Figure 8, one notes a significant difference in resolution of the deuterium second harmonic in the echo envelope which depends on the proximity to the copper centers. In Figure 8A, the trace for equatorially bound D_2O, the second harmonic is more prominent than for axial D_2O (trace B), where the deuterium is further removed from the copper. For ambient D_2O (Figure 8C) the second harmonic is not resolved at all. An examination of the ratio of modulation data for the mercury derivative of laccase in D_2O and H_2O clearly demonstrates a resolved second harmonic, once again suggesting the presence of equatorial water as a ligand to copper.

We can further use the ratio technique to determine from which position water is displaced when azide binds to the copper in the active site. A ratio of the modulation patterns of enzyme samples in D_2O and H_2O provides us with those modulations of deuterium present on copper ligands or as a replacement for solvent-exchangeable protons on the protein (Figure 9A). A second ratio is obtained from two samples of the azide bound enzyme, again, in D_2O and H_2O (Figure 9B). This second ratio provides the same deuterium modu-

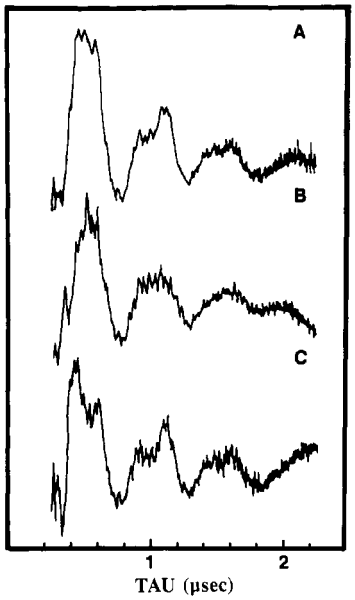

FIGURE 9: Deuterium modulation arising from water displaced by azide binding to copper in the mercuric derivative of laccase. Trace A is the ratio of two-pulse modulation data for the protein in D_2O and H_2O. Trace B is the ratio of modulations of identical samples of protein in D_2O and in H_2O that had been treated with $^{15}N_3^-$. Trace C is the ratio of trace B divided by trace A and represents the deuterium modulation of azide-displaced D_2O. Two-pulse ESEEM data were collected at 3050 G at a microwave frequency of 8.84 GHz.

lations described above less those of the putative water ligand displaced by azide. The ratio of these two resultant deuterium modulation patterns leaves us with the deuterium modulation of any putative displaced water (Figure 9C). This deuterium modulation closely resembles that obtained for equatorially bound water (Figure 8A), and we conclude that it is from this position that water is displaced from the type 2 site in laccase when azide is bound.

Conclusion. We have presented EPR and electron spin-echo data that we have used to determine the coordination properties of the type 2 copper site in the mercury derivative of laccase. On the basis of the ESEEM of the protein, we determined that minimally two imidazoles are equatorially bound to copper, although the data do not preclude another axially or equatorially coordinated nitrogenous ligand.

Using both two- and three-pulse ESEEM methods, water is shown to be accessible to the copper site, on the basis of deuterium-exchange experiments. Its direct coordination to copper is suggested. When azide binds to the metal, it displaces a water at the equatorial position.

From the results presented, it is interesting to note that the ligation proposed here for the type 2 copper in the mercury derivative of laccase bears a resemblance, both in the number of imidazoles coordinated and in the water ligation, to the type 2 site in ascorbate oxidase as determined by X-ray crystallographic analysis (Messerschmidt et al., 1989). On the basis of an alignment of amino acid sequences of ascorbate oxidase with those for the related proteins laccase and ceruloplasmin, similar bis(imidazole) coordination to the type 2 copper in these proteins is suggested (Messerschmidt & Huber, 1990). A similar comparison of amino acid alignments of the Messerschmidt and Huber data and nitrite reductase has been performed (Fenderson et al., 1991) and specific motifs of copper ligands are conserved among these proteins. It would appear, then, that the ligand composition of each type of copper in the multinuclear, blue copper oxidase is constant and may have structural analogy with corresponding sites in proteins where only one type of copper is present. So, the type 1 copper in ascorbate oxidase has identical ligand composition with the mononuclear copper proteins azurin (Adman et al., 1978) and plastocyanin (Colman et al., 1978) [but not stellacyanin (Peisach et al., 1967; Bergman et al., 1977)], while the type 3 copper of ascorbate oxidase structurally resembles the binuclear center in hemocyanin (Gaykema et al., 1984). For those copper proteins containing only type 2 copper, the number of imidazoles coordinated to metal is minimally two, such as found in galactose oxidase (Ito et al., 1991), but can be as many as four, such as in superoxide dismutase (Richardson et al., 1975). In all instances, though, specificity of metal binding for all divalent copper centers requires imidazole coordination.

REFERENCES

Adman, E. T., Stenkamp, R. E., Sieker, L. C., & Jensen, L. H. (1978) *J. Mol. Biol. 123*, 35–47.

Avigliano, L., Davis, J. L., Graziani, M. T., Marchesini, A., Mims, W. B., Mondovi, B., & Peisach, J. (1981) *FEBS Lett. 136*, 80–84.

Bergman, C., Gandvik, E. K., Nyman, P. O., & Strid, L. (1972) *Biochem. Biophys. Res. Commun. 77*, 1052–1059.

Blumberg, W. E., & Peisach, J. (1987) *Life Chem. Rep. 5*, 5–36.

Branden, R., & Deinum, J. (1977) *FEBS Lett. 73*, 144–146.

Branden, R., Malmstrom, B. G., & Vanngard, T. (1973) *Eur. J. Biochem. 36*, 195–200.

Britt, R. D., & Klein, M. P. (1987) *J. Magn. Reson. 74*, 535–537.

Colman, P. M., Freeman, H. C., Guss, J. M., Murata, M., Norris, V. A., Ramshaw, J. A. M., & Venkatappa, M. P. (1978) *Nature 272*, 319–324.

Cornelius, J. B., McCracken, J., Clarkson, R. B., Belford, R. L., & Peisach, J. (1990) *J. Phys. Chem. 94*, 6977–6982.

Fenderson, F. F., Kumar, S., Adman, E. T., Liu, M.-Y., Payne, W. J., & LeGall, J. (1991) *Biochemistry 30*, 7180–7185.

Froncisz, W., & Aisen, P. (1982) *Biochim. Biophys. Acta 700*, 55–58.

Gaykema, W. P. J., Hol, W. G. J., Vereijken, J. M., Soeter, N. M., Bak, H. J., & Beintema, J. J. (1984) *Nature 309*, 23–29.

Graziani, M. T., Morpurgo, L., Rotilio, G., & Mondovi, B. (1976) *FEBS Lett. 70*, 87–90.

Hyde, J. S., & Froncisz, W. (1982) *Annu. Rev. Biophys. Bioeng. 11*, 391–417.

Hyde, J. S., Rist, G. H., & Eriksson, L. E. G. (1968) *J. Phys. Chem. 72*, 4269–4276.

Ito, N., Phillips, S. E. V., Stevens, C., Ogel, Z. B., McPherson, M. J., Keen, J. N., Yadav, K. D. S., & Knowles, P. F. (1991) *Nature 350*, 87–90.

Jiang, F., McCracken, J., & Peisach, J. (1990) *J. Am. Chem. Soc. 112*, 9035–9044.

Kevan, L., & Kispert, L. D. (1976) *Electron Spin Double Resonance Spectroscopy*, Wiley, New York.

Klemens, A. S., McMillin, D. R., Tsang, H. R., Penner-Hahn, J. E. (1989) *J. Am. Chem. Soc. 111*, 6398–6402.

Kosman, D., Peisach, J., & Mims, W. B. (1980) *Biochemistry 19*, 1304–1308.

Lin, C. P., Bowman, M. K., & Norris, J. R. (1985) *J. Magn. Reson. 65*, 369–374.

Malmstrom, B. G., Reinhammar, B., & Vanngard, T. (1968) *Biochim. Biophys. Acta 156*, 67–76.

McCracken, J., Peisach, J., & Dooley, D. M. (1987) *J. Am. Chem. Soc. 109*, 4064–4072.

McCracken, J., Pember, S., Benkovic, S. J., Villafranca, J. J., & Peisach, J. (1988) *J. Am. Chem. Soc. 110*, 1069–1074.

McMillin, D. R., Rosenberg, R. C., & Gray, H. B. (1974) *Proc. Natl. Acad. Sci. U.S.A. 71*, 4760-4762.
Messerschmidt, A., & Huber, R. (1990) *Eur. J. Biochem. 187*, 341-352.
Messerschmidt, A., Rossi, A., Ladenstein, R., Huber, R., Bolognesi, M., Gartti, G., Marchesini, A., Petruzzelli, R., & Finazzi-Agro, A. (1989) *J. Mol. Biol. 206*, 513-529.
Mims, W. B. (1972) *Phys. Rev. 135*, 2409-2419.
Mims, W. B. (1984) *J. Magn. Reson. 59*, 291-306.
Mims, W. B., & Peisach, J. (1978) *J. Chem. Phys. 69*, 4921-4930.
Mims, W. B., & Peisach, J. (1989) in *Advanced EPR in Biology and Biochemistry* (Hoff, A., Ed.) pp 1-57, Elsevier, Amsterdam.
Mims, W. B., Peisach, J., & Davis, J. (1977) *J. Chem. Phys. 66*, 5536-5550.
Mims, W. B., Davis, & Peisach, J. (1984) *Biophys. J. 45*, 755-766.
Mondovi, B., Graziani, M. T., Mims, W. B., Oltzik, R., & Peisach, J. (1977) *Biochemistry 16*, 4198-4202.
Morie-Bebel, M., Morris, M. C., Menzie, J. L., & McMillin, D. R. (1984) *J. Am. Chem. Soc. 106*, 3677-3678.
Morie-Bebel, M., McMillin, D. R., & Antholine, W. E. (1986) *Biochem. J. 235*, 415-420.
Norris, G. E., Anderson, B. F., & Baker, E. N. (1981) *J. Mol. Biol. 165*, 501-521.
Peisach, J., & Blumberg, W. E. (1974) *Arch. Biochem. Biophys. 165*, 691-708.
Peisach, J., Levine, W. L., & Blumberg, W. E. (1967) *J. Biol. Chem. 242*, 2847-2858.
Reinhammar, B. (1972) *Biochim. Biophys. Acta 275*, 245-259.
Reinhammar, B. (1984) in *Copper Proteins and Copper Enzymes* (Lontie, R., Ed.) Vol. III, pp 1-36, CRC Press, Boca Raton, FL.
Richardson, J. S., Thomas, K. A., Rubin, B. H., & Richardson, D. C. (1975) *Proc. Natl. Acad. Sci. U.S.A. 72*, 1349-1353.
Roberts, J. E., Cline, J. F., Lum, V., Freeman, H., Gray, H. B., Peisach, J., Reinhammar, B., & Hoffman, B. M. (1984) *J. Am. Chem. Soc. 106*, 5324-5330.
Solomon, E. I. (1981) in *Copper Proteins* (Spiro, T. G., Ed.) pp 41-108, Wiley, New York.
Solomon, E. I., Hare, J. W., & Gray, H. B. (1976a) *Proc. Natl. Acad. Sci. U.S.A. 73*, 1389-1393.
Solomon, E. I., Dooley, D. M., Wang, R.-H., Gray, H. B., Cerdonio, M., Mogno, F., & Romani, G. L. (1976b) *J. Am. Chem. Soc. 98*, 1029-1031.
Tsvetkov, Yu. D., & Dikanov, S. A. (1987) *Met. Ions Biol. Syst. 22*, 207-263.

Co^{2+} as a Shift Reagent for ^{35}Cl NMR of Chloride with Vesicles and Cells†

Yair Shachar-Hill*,‡ and Robert G. Shulman
Department of Chemistry, Yale University, New Haven, Connecticut 06511
Received January 24, 1992; Revised Manuscript Received April 21, 1992

ABSTRACT: Applications of high-resolution ^{35}Cl NMR to the study of chloride in vivo and in vesicles have hitherto been limited by problems of NMR detectability and of resolving internal from external signals. We have characterized the effects of Co^{2+} on the ^{35}Cl resonance of Cl^- in solution and have shown that when added to suspensions of lipid vesicles, Co^{2+} shifts the ^{35}Cl signal of the extravesicular Cl^-, allowing clear resolution and quantitation of two peaks. We have assigned these signals to chloride inside and outside the vesicles. The spectra do not change over a 90-min period, demonstrating the stability of the vesicles in the presence of Co^{2+}. This technique is shown to be applicable to red blood cell ghosts, where intravesicular and extravesicular chloride signals were separated and measured and chloride/sulfate exchange through the band 3 anion transport protein A was followed. In two plant species (an alga and a higher plant), an intracellular Cl^- signal can be observed and resolved from the extracellular signal. The intracellular transportable chloride was found to be fully NMR-visible (±5%) in the algal cells. The high steady-state levels of Cl^- seen in the alga were consistent with previous work using $^{36}Cl^-$ labeling on a related species [Doblinger, R., & Tromballa, H. W. (1982) *Planta 156*, 10-15]. Successive spectra acquired after adding Co^{2+} to *Chlorella* cells under deenergizing conditions allow us to follow the time course of movement of Cl^- out of the cells.

High-resolution ^{35}Cl NMR has been used in inorganic chemical studies of the interaction of Cl^- with metal ions and complexes in solution [reviewed by Lindman and Forsén (1976)] and in many investigations of chloride binding to proteins, both in solution [reviewed by Forsén and Lindman (1981)] and with integral membrane proteins (Baianu et al., 1984; Shami et al., 1977; Falke et al., 1984a,b; Shachar-Hill et al., 1989). However, the application of ^{35}Cl NMR to studying chloride in vivo has been restricted by two problems: the superposition of the signals from intra- and extracellular chloride and the fact that in all cells studied to date intracellular signals are too broad to quantify. This has been found in human red blood cells (Falke et al., 1984b; Brauer et al., 1985; Hoffman & Gupta, 1987), rat proximal tubules (Hoffman et al., 1987), and *Escherichia coli* (this study). This broadening of intracellular signals is due to the very rapid quadrupolar relaxation of the ^{35}Cl nucleus when its motion is restricted by binding to a protein or other slowly tumbling species where electric field gradients at the ^{35}Cl nucleus are

† This work was supported by NSF Grant DBM 861630.
* Author to whom correspondence should be addressed.
‡ Present address: Department of Biochemistry, Cambridge University, Cambridge CB2 1QW, England.

0006-2960/92/0431-6272$03.00/0